# STUDY OF TEMPERATURE DEPENDENCE OF PHYSICAL PROPERTIES OF ZINC OXIDE BY RAMAN SPECTROSCOPY

<sup>1</sup>U.Kh. Kholikov, <sup>2\*</sup>Sh.Yu. Menglieva, <sup>2</sup>I.O. Kosimov, <sup>2,3</sup>Sh.T. Khozhiev, <sup>4</sup>I.Kh. Khudaykulov, <sup>4</sup>U.F. Berdiyev, <sup>5</sup>E.A. Yolchueva, <sup>5</sup>L.A. Hasanova

> Received 17.03.2025 Accepted 08.05.2025

Abstract: This research examines the effect of annealing temperature on the phase, optical, and structural characteristics of ZnO nanopowder. Characterization of samples was carried out using a combination of Raman spectroscopy, scanning electron microscopy (SEM), UV-visible spectroscopy, and X-ray diffraction (XRD) methods. The degrees of amorphousness and crystallinity were determined using the Search Match 3 software. The Raman spectroscopy method revealed significant changes in the shape, orientation, and distribution of ZnO nanopowder peaks formed with increasing annealing (heating) temperature, as well as explaining the phonon oscillation mode. The obtained high intensity of Raman scattering confirmed the high-frequency phonon mode of hexagonal wurtzite ZnO. The structural images of the sample were obtained by scanning electron microscopy.

**Keywords:** heterostructures, phonon vibration mode, Raman scattering, longitudinal optical (LO)-transverse optical (TO) frequencies of background modes-peaks, wurtzite

### Introduction

Zinc oxide (ZnO) is a compound with remarkable physical and chemical properties that make it highly suitable for a variety of nanotechnology applications. Its wide band gap of about 3.37 eV enables efficient light emission useful in optoelectronics, such as ultraviolet light sources and photodetectors [1–3]. Some of these applications include biomedicine, energy, sensors, and optics. As research on ZnO nanostructures continues to grow, it has inspired several new innovative applications [4-5]. In addition to its distinctive chemical properties, zinc oxide (ZnO) benefits from straightforward crystal growth techniques and significantly reduces production costs compared to other semiconductors utilized in nanotechnology. Various synthesis methods have been developed to produce high-quality ZnO nanostructures, particularly nanowires. These processes enable the efficient fabrication of ZnO with tailored properties, enhancing its application potential in diverse technological fields. ZnO possesses a strong exciton binding energy of about 60 meV at room temperature and a thermally stable hexagonal wurtzite crystal structure. These physical characteristics, coupled with its highly efficient light-absorbing and emitting nature, render ZnO very promising to fabricate functional materials for next-generation optoelectronic, photonic and energy harvesting devices. In addition, ZnO is also radiation-resistant and aggressive chemical environments-resistant, as well as being wet-etching-compatible, which makes it an ideal choice for microfabrication processes. Its oxidation properties are also highly potent, which further increases its catalytic attributes. Because of these properties, ZnO is also discovered to have a broad array of uses in solar cells, transparent conducting coatings, spintronics devices, laser deflectors, antimicrobial coatings, gas sensors, piezoelectric devices and biosensors. Its low price, ease of availability, and simplicity of processing are also reasons for its popularity as a crucial element of research and industrial technology [6-10]. To expand the possibilities of using ZnO in various

devices and components, numerous attempts have been made to modify its optical and/or electrical properties using doping, ion irradiation, and other methods. This is because, in its unchanged form, ZnO, as a rule, has low activity in charge carrier transfer and insufficient efficiency in absorbing solar radiation, which limits its use without additional processing. For example, when using ZnO as a photocatalyst for accelerated decomposition of organic pollutants, the photocatalytic process can only be started under the influence of ultraviolet radiation, which makes up less than 5% of the solar spectrum on the Earth's surface. This is because the boundary of its light absorption is determined by a wide band gap. One of the promising approaches to extending the light absorption range to the visible spectrum is the alloying of ZnO with metals, which makes it possible to modify its band gap. In addition, such metal additives can capture electrons, thereby increasing the lifetime of photogenerated electron-hole pairs [11-13]. On the other hand, when using ZnO in optoelectronics, one of the main problems is the difficulty of obtaining high-quality ZnO powder with p-type conductivity. This is due to the self-compensation effect, which causes an internal defect in the crystal lattice, as well as low solubility and inactivation of acceptor impurities in the ZnO structure. In the context of the rapid development of nanoelectronics, the importance of optical research methods is increasing, especially the importance of using Raman light scattering.

In this work, we investigated the phase states of powdered ZnO subjected to annealing at temperatures from 200 °C to 700 °C. The results obtained, along with our previous work [14, 15], confirm that the Raman spectroscopy method provides an opportunity to perform both qualitative and quantitative analysis of both the surface and volume of samples, allows us to study the structure of films, register defects and internal stresses, and track the phase identification between the amorphous and crystalline states of matter.

## **Experimental part**

In the research, ZnO powder samples were heat-treated at three temperatures to investigate heat treatment-induced structural and phase changes. Raman spectroscopy and X-ray powder diffractometry (XRD) have been used as the leading analytical methods to identify the changes. The degrees of amorphousness and crystallinity were determined using the Search Match 3 software. Using Raman spectroscopy, significant changes were found in the shape, orientation, and peak distribution of ZnO nanopowders formed with increasing annealing (heating) temperature. The presence of intense Raman scattering in ZnO powder samples indicates the existence of a longitudinal optical phonon mode. Small shifts were found in all ZnO modes, which indicate the presence of stress and strain in the crystal lattice. Changes in particle size were studied using confocal Raman microscopy during thermal annealing. It is shown that changes in the structure and particle sizes of the material have improved its characteristics. It is confirmed that nanocomposite heterostructures obtained by a simple chemical method are applicable for creating optoelectronic devices. The use of the Raman scattering method makes it possible to obtain a wide range of physical characteristics of the material under study due to regular changes in the scattering spectra [16-18]. Raman spectroscopy has proven to be a fast and non-destructive analysis method for using nanocrystal size identification, phase ratio estimation, crystal lattice composition analysis, and for detecting deformations and internal stresses based on the analysis of the position and shape of peaks in the light scattering spectrum [19].

In the framework of this study, spectral measurements were performed using an inVia Raman microspectrometer (Renishaw, UK) equipped with an RL785 class 3B laser with a wavelength of 785 nm. A diffraction grating with a frequency of 1200 lines/mm was used as a dispersing element, and the signal was recorded by a standard Renishaw CCD camera [20-22].

To study the morphological features of the ZnO samples, scanning electron microscopy (SEM) was used on a JSM-IT210 instrument, and the elemental composition was analyzed by energy dispersive X-ray spectroscopy (EDX). The concentrations of chemical elements in the composites were measured using electron probe X-ray spectral microanalyzers for energy-dispersive X-ray analysis (EDXA) as part of the SEM.

**Sample production method.** Zinc oxide nanoparticles were synthesized by precipitation from solution. The process of obtaining ZnO is based on the reaction between zinc acetate dehydrate and sodium carbonate, which results in the formation of zinc oxide in the form of a precipitate. The chemical reaction proceeds according to the following scheme:

$$Zn(CH_3COO)_2 \cdot 2H_2O + Na_2CO_3 \rightarrow ZnO\downarrow + 2CH_3COONa + CO_2\uparrow + 2H_2O$$

To carry out the synthesis, a 0.1 M solution of zinc acetate was gradually added to a 5% solution of polyvinyl alcohol while stirring on a magnetic stirrer for 30 minutes. After that, 0.1 M sodium carbonate solution was introduced into the system, and stirring continued for another 15 minutes at room temperature. The formed ZnO precipitate was separated by centrifugation at 3500 rpm, washed with deionized water, and dried at room temperature.

#### Results and discussion

In this work, the morphological, optical, electrical, and structural properties as a function of the annealing temperature from 200 °C to 700 °C were investigated using Raman spectroscopy, UV-Vis spectroscopy, and X-ray powder diffraction (XRD), respectively. UV-visible spectroscopy similarly showed that ZnO samples irradiated at different temperatures had band gaps ranging from 3.46 to 3.35 eV. The values of the film resistivity obtained from the I–V characteristics showed an exponential increase in resistivity with increasing annealing temperature of the ZnO sample.

Raman spectra. Fig.s 1 and 2 show the Raman spectra of the nanostructures, as well as an image of a section of the surface of the studied ZnO sample. As can be seen from the data provided for the initial sample, the intensity of the peak at -438 cm<sup>-1</sup> is 42000; subsequent annealing at a temperature of 200°C leads to a decrease in the intensity of this peak to 24000, and at a temperature of 500°C 20000. This indicates that with an increase in temperature to 500°C the intensity decreases. At an annealing temperature of 700 °C, the intensity of this peak increases sharply to 56000. This nature of the growth of this peak indicates that annealing will first lead to the decomposition of nanolayers, and further annealing will again lead to the ordering of the sample structure. A similar picture is observed when analyzing other characteristics of this ZnO material. To simplify the interpretation of the results, the spectra were conditionally divided into two regions: from 200 to 510 cm<sup>-1</sup> and from 530 to 1300 cm<sup>-1</sup>, as shown in Fig. 1 and 2. In the low-frequency region, characteristic ZnO peaks were recorded at 331, 383, and 436 cm<sup>-1</sup>. In the high-wavenumber region, peaks were also noted at 584, 660, 1101, and 1154 cm<sup>-1</sup>.

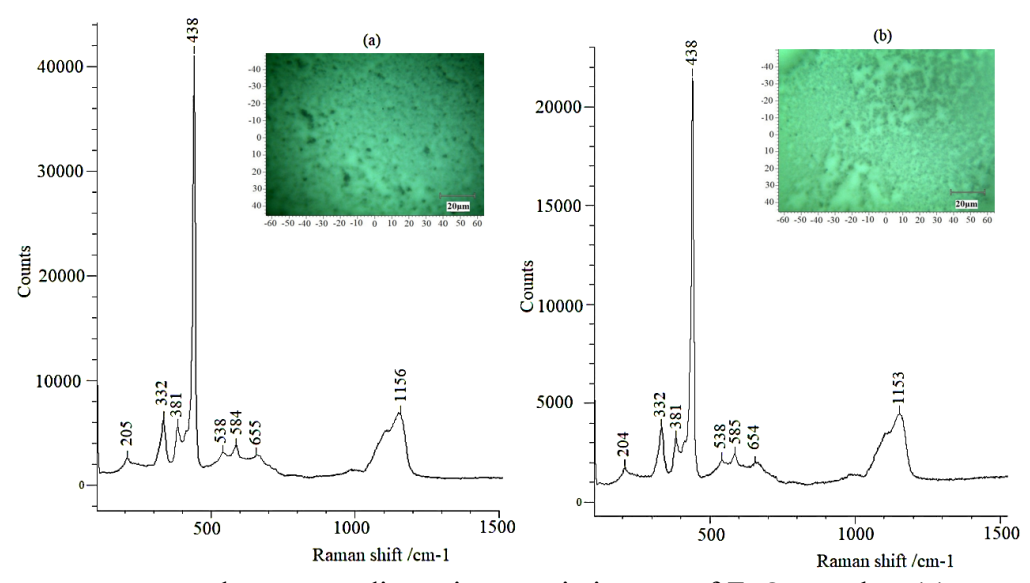


**Fig. 1.** Raman spectra and corresponding microscopic images of ZnO samples: **(a)** as-synthesized ZnO (unannealed); **(b)** ZnO annealed at 200 °C.

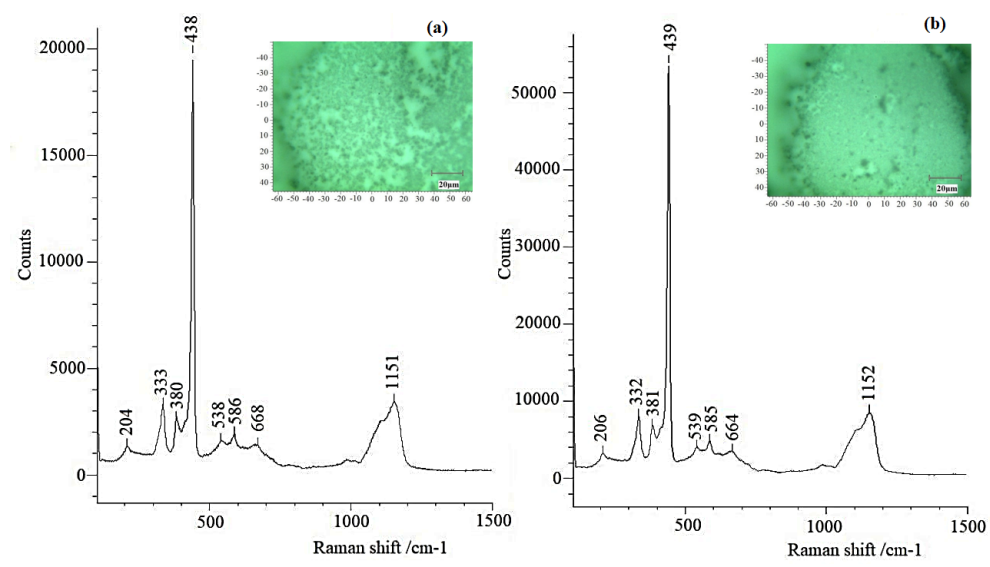


**Fig. 2.** Raman spectra and corresponding microscopic images of ZnO samples: **(a)** ZnO annealed at 500 °C; **(b)** ZnO annealed at 700 °C.

The peaks at 352 cm<sup>-1</sup> and 654 cm<sup>-1</sup> can be attributed to the A<sub>1</sub> symmetry modes. The peak at 438 cm<sup>-1</sup> corresponds to non-polar optical phonons of ZnO, related to the high E<sub>2</sub> mode. The peak at 381 cm<sup>-1</sup> is interpreted as a mode of A<sub>1</sub> symmetry associated with the transverse optical (TO) phonon regime. Peaks at 585 and 1154 cm<sup>-1</sup> – E<sub>1</sub> symmetry corresponds to the longitudinal optical modes LO and 2LO, respectively. In addition, the intensities of all observed vibrational modes decrease with increasing annealing temperature to 500°C and then increase again at an annealing temperature of 700°C. As a result, the size of the nanostructures decreases. In addition, their line shapes become asymmetrical.

**Electron-phonon relationship.** It is well known that as particle sizes decrease to the nanoscale or as crystal lattice distortions increase, the effect of the k=0 selection rule for first-order Raman scattering weakens. This leads to the fact that phonon scattering is no longer limited to the center of the Brillouin zone. In this regard, it becomes important to take into account the phonon dispersion near the zone center. Such a deviation from the ideal case is accompanied not only by a shift and broadening of the scattering bands corresponding to first-order optical phonons, but can also lead to the manifestation of modes with forbidden symmetry.

In this study, we present results concerning the electron-phonon interaction obtained from Raman scattering (RS) data, which have previously been practically not considered for ZnO nanopowders. The ratio between the second- and first-order scattering cross sections turned out to be very sensitive to the degree of electron-phonon interaction [22, 23]. For bulk ZnO, this ratio between the intensities of the E<sub>1</sub>(2LO) and E<sub>1</sub>(LO) modes was calculated as 2.85 [21], which is confirmed by the observed peaks corresponding to these combination modes. Thus, as can be seen from the presented data, phonon scattering is still limited to the region of the center of the Brillouin zone, but the intensity ratio between the second- and first-order scattering increases significantly. The broad peak in the region of 560-610 cm<sup>-1</sup> with a maximum of about 574 cm<sup>-1</sup> corresponds to lattice vibrations in the E<sub>1</sub>(LO) mode in pure ZnO. This mode is characteristic of crystallites with arbitrary crystallographic orientation [21] and is caused by the presence of internal defects such as oxygen vacancies, interstitial zinc atoms, and resonance effects at a certain excitation wavelength in the ZnO crystal lattice [22, 23]. These features indicate the presence of compressive stresses in the structure, typical of heterostructured materials. The E<sub>1</sub> and A<sub>1</sub> modes are both Raman and infrared active, since they manifest themselves in longitudinal (LO) and transverse (TO) optical vibrations [23]. Additionally, peaks at 333, 382, 417–424, and 574 cm<sup>-1</sup> were recorded in the ZnO spectra, which correspond to the E2 H - E2L, A<sub>1</sub>(TO), E<sub>1</sub>(TO), and E<sub>1</sub>(LO) modes, respectively. These modes exhibit frequency shifts in the Raman spectra, which further confirms the presence of LO phonon modes and indicates the existence of a characteristic morphology associated with the heterostructure.

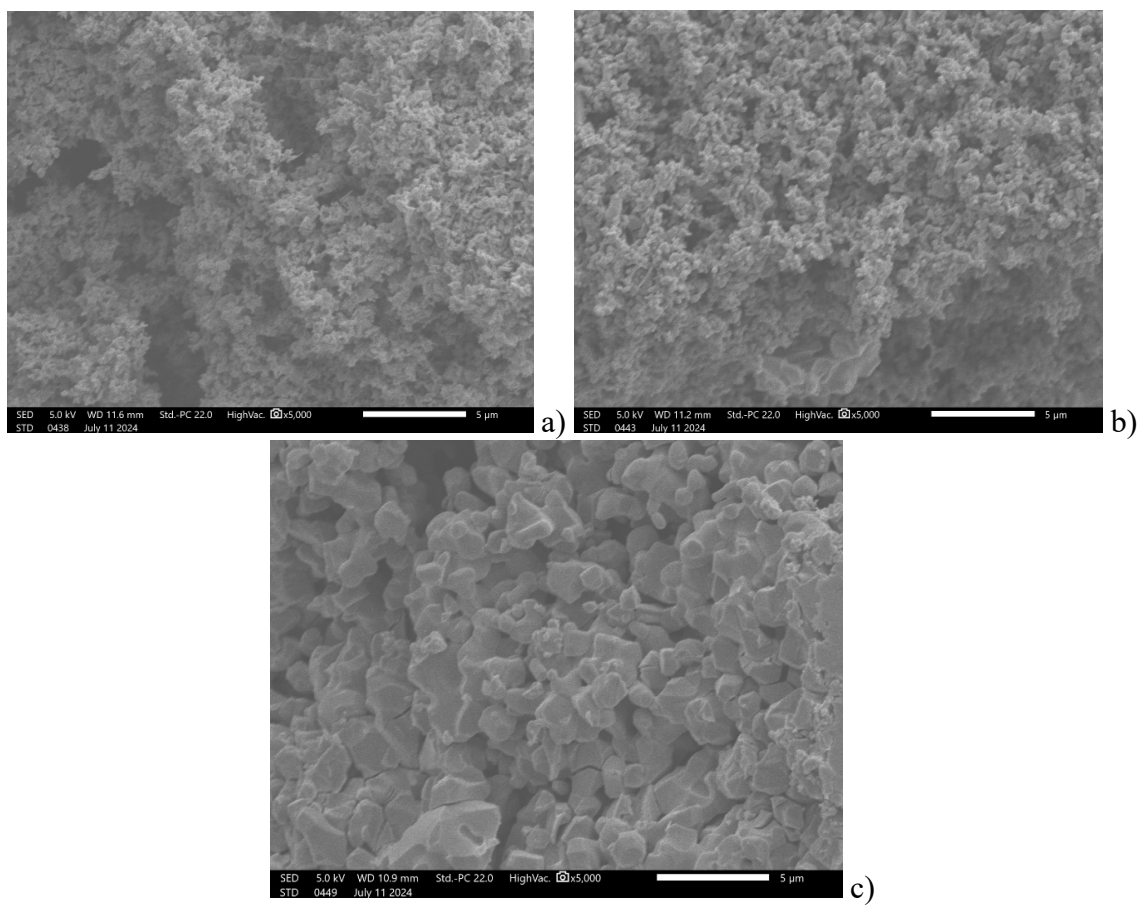


**Fig. 3.** SEM images of the ZnO sample surface at different annealing temperatures: (a) the initial (as-prepared) state, (b) after annealing at 700 °C, and (c) after annealing at 1100 °C.

Fig. 3 shows typical SEM images of ZnO nanopowder surface morphology. It can be seen that thermal annealing causes evident grain growth with particle sizes from a few micrometers to some tens of micrometers (Fig. 3a–c). As mentioned above, elemental composition of the samples was also investigated using energy-dispersive X-ray spectroscopy (EDX). As shown in the EDS spectra (Fig. 4), the samples exhibit strong Zn and O peaks, indicating the presence of pure ZnO phases with minimal impurity levels.

Table 1. Elemental composition of ZnO sample based on EDX analysis

ZAF

Quantification method

Result Type

Metal

Standard data

Standardless

Display name

Spc\_001

Element	Line	Mass%	Atom%
C	K	2.01±0.03	8.88±0.13
0	K	4.40±0.04	14.63±0.12
Al	K	0.30±0.01	0.59±0.02
Zn	K	93.29±0.26	75.90±0.21
Total		100.00	100.00
Spc_001 Fitting ratio 0.00			Fitting ratio 0.0045

The atomic ratio between zinc and oxygen in the synthesized nanopowders was determined using EDX, and the main results are shown in Table 1. The analysis showed that oxygen deficiency was observed in all the samples studied. Nevertheless, taking into account the possible

measurement error of light elements such as oxygen, it can be argued that the obtained values are generally close to the stoichiometric ratio.

ZnLb
ZnKa

ZnKa

All2,3
CKa
OKa
OKa
AlKa
O

Senergy [keV]

Fig.4. Energy-dispersive X-ray spectra (EDS) of ZnO samples.

In addition, we also discovered in Fig. 4 the presence of carbon and aluminum in the composition of zinc oxide nanopowder. Despite this, as the results of the SEM-EDS analysis show, the sample prepared in the above manner contains pure ZnO phases.

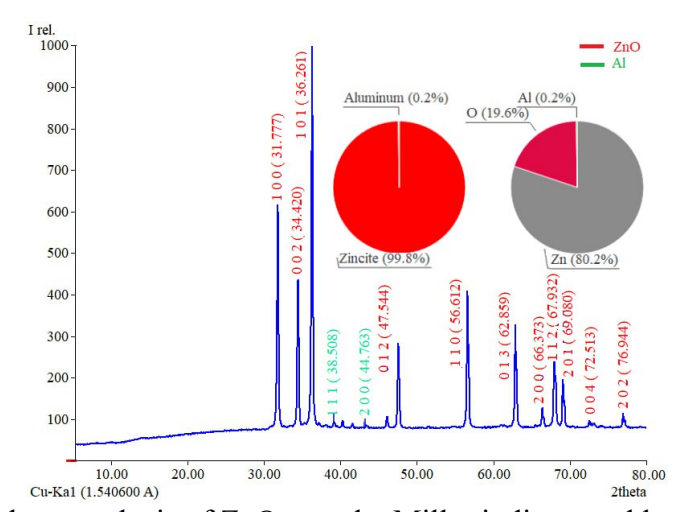


Fig. 5. X-ray phase analysis of ZnO sample, Miller indices, and lattice parameters.

X-ray analysis showed that the ZnO samples have a hexagonal wurtzite ZnO structure with peaks at 2θ-positions of 31.7°, 34.4°, 36.2°, 47.5°, 56.6°, and 62.8°, belonging to the planes (100), (002), (101), (012), (110), and (013), respectively (Fig. 5). We also determined the Miller indices and lattice parameters. We also conducted phase quantitative and qualitative analyses of ZnO nanopowders. The obtained experimental data are in good agreement with the data obtained by other methods. The degree of crystallinity and the content of the amorphous phase in the ZnO samples were estimated by X-ray diffraction analysis using the *Search* and *Match 3* software. According to the data obtained, the proportion of the amorphous phase in the sample under study was 86.27%, while the crystalline phase was 13.73%. It was also found that with an increase in the annealing temperature, an increase in the degree of crystallinity of ZnO was observed, indicating a gradual ordering of the material structure during heat treatment.

#### Conclusion

Thus, the Raman spectra of ZnO nanocrystals showed that the strength of the electron-phonon interaction increases with the increase in the size of the nanocrystals when heated to 700°C. The intense E<sub>2</sub>H peak (high-frequency phonon mode) at 438 cm<sup>-1</sup> indicates the presence of a wurtzite-type hexagonal crystal structure, which is characteristic of highly crystalline ZnO. This non-polar mode is associated with vibrations of the heavy zinc sublattice and oxygen atoms. The E<sub>2</sub>H peak is

characterized by a relatively high intensity compared to other modes and a narrow and distinct shape, which is typical of pure and well-crystallized ZnO. Changes in particle size were also detected using confocal Raman microscopy upon thermal annealing. It was shown that changes in the structure and particle sizes of the material improved its characteristics. Oxygen deficiency was also detected for all samples, and the compositions were maintained within the stoichiometry limits, taking into account the measurement error of the light element oxygen. In addition, we determined the presence of carbon and aluminum in the composition of zinc oxide nanopowder. It has been confirmed that nanocomposite heterostructures obtained by a simple chemical method apply to the creation of optoelectronic devices.

#### References

- 1. Steglich M., Bingel A., Jia G., Falk F. Atomic layer deposited ZnO: Al for nanostructured silicon heterojunction solar cells. *Sol. Energy Mater. Sol. Cells.* 2012, **Vol. 103**, p. 62–68. DOI: 10.1016/j.solmat.2012.04.004
- 2. Lu T.C., Lai Y.Y., Lan Y.P., Huang S.W., Chen J.R., Wu Y.C., Hsieh W.F., Deng H. Room temperature polariton lasing vs. photon lasing in a ZnO-based hybrid microcavity. *Opt. Express*. 2012, **Vol. 20**, p. 5530–5537. DOI: 10.1364/OE.20.005530
- 3. Wang L., Kang Y., Liu X., Zhang S., Huang W., Wang S. ZnO nanorod gas sensor for ethanol detection. *Sens. Actuators B Chem.* 2012, **Vol. 162**, p. 237–243. DOI: 10.1016/j.snb.2011.12.073
- 4. Ho C.C., Lai L.W., Lee C.T., Yang K.C., Lai B.T., Liu D.S. Transparent sputtered ITO-ZnO electrode ohmic contact to n-type ZnO for ZnO/GaN heterojunction light-emitting diode. *J. Phys. D Appl. Phys.* 2013, **Vol. 46**, 315102. DOI: 10.1088/0022-3727/46/31/315102
- 5. Ibupoto Z.H., Khun K., Eriksson M., AlSalhi M., Atif M., Ansari A., Willander M. Hydrothermal growth of vertically aligned ZnO nanorods using a biocomposite seed layer of ZnO nanoparticles. *Materials*. 2015, Vol. 6, p. 3584–3597. DOI: 10.3390/ma6083584
- 6. Hu J.T., Odom T.W., Lieber C.M. Chemistry and physics in one dimension: Synthesis and properties of nanowires and nanotubes. *Acc. Chem. Res.* 1999, **Vol. 32**, p. 435–445. DOI: 10.1021/ar9700365
- 7. Iijima S. Helical microtubules of graphitic carbon. *Nature*. 1991, **Vol. 354**, p. 56–58. DOI:10.1038/354056a0
- 8. Feldman Y., Wasserman E., Srolovitz D.J., Tenne R. High-rate, gas-phase growth of MoS<sub>2</sub> nested inorganic fullerenes and nanotubes. *Science*. 1995, **Vol. 267**, p. 222–225. DOI: 10.1126/science.267.5195.222
- 9. Yan Y., Zhang S.B., Pantelides S.T. Control of doping by impurity chemical potentials: Predictions for p-type ZnO. *Phys. Rev. Lett.* 2001, **Vol. 86**, p. 5723–5726. DOI: 10.1103/PhysRevLett.86.5723
- 10. Cao H., Zhao Y.G., Ho S.T., Seelig E.W., Wang Q.H., Chang R.P.H. Random laser action in semiconductor powder. *Phys. Rev. Lett.* 1999, **Vol. 82**, p. 2278–2281. DOI: 10.1103/PhysRevLett.82.2278
- 11. Wiersma D. The smallest random laser. *Nature*. 2000, **Vol. 406**, p. 132–133. DOI: 10.1038/35018184
- 12. Vayssieres L., Keis K., Lindquist S.-E., Hagfeldt A. Purpose-built anisotropic metal oxide material: 3D highly oriented microrod array of ZnO. *J. Phys. Chem. B.* 2001, **Vol. 105**, p. 3350–3352. DOI: 10.1021/jp010026s
- 13. Li Y., Meng G.W., Zhang L.D., Phillipp F. Ordered semiconductor ZnO nanowire arrays and their photoluminescence properties. *Appl. Phys. Lett.* 2000, **Vol. 76**, p. 2011–2013. DOI: 10.1063/1.126238
- 14. Khoziev Sh.T., Rotshtein V.M., Ashurov R.Kh., Ganiev A.A. Study of photoluminescence spectra of zinc selenide samples by Raman spectroscopy. *Universum: Technical Sciences*, 2020, Vol. 73(4), 4 pages.

- 15. Khoziev Sh.T., Rotshteyn V.M., Pak S.S. Study of silicon doped with boron ions by Raman spectroscopy. *Higher School. Scientific and Practical Journal*. 2020, **No.3**.
- 16. Levitt A.P. Whisker Technology. Wiley-Interscience. New York. 1970.
- 17. Yang P., Lieber C.M. Nanorod-superlattice-based photonic crystal. *Nature*, 2002, **Vol. 419**, p. 553.
- 18. Park W.I., Kim D.H., Jung S.W., Yi G.C. Metalorganic vapor-phase epitaxial growth of vertically well-aligned ZnO nanorods. *Appl. Phys. Lett.* 2002, **Vol. 80**, p. 4232. DOI: 10.1063/1.1482800
- 19. Sears G.W. Kinetics of the growth of colloidal particles. *Acta Metall.* 1955, Vol. 4, p. 361.
- 20. Klein M.C., Hache F., Ricard D., Flyzanis C. Size dependence of ultrafast electronic dephasing in semiconductor nanocrystals. *Phys. Rev. B.* 1990, **Vol. 42**, 11123.
- 21. Menglieva S., Khozhiev S., Usmanova Z., Tukhtaev K. The technology of green synthesis of calcium acetate from quail egg shells. *BIO Web of Conf.* 2024, **Vol. 82**, 04001. DOI:10.1051/bioconf/20248204001
- 22. Wang R.P., Xu G., Jin P. Structural and optical properties of ZnO thin films prepared by pulsed laser deposition. *Phys. Rev. B.* 2004, **Vol. 69**, 113303. DOI: 10.3390/cryst10020132
- 23. Rati I., Rini A.S., Akrajas A.U., Agustin M. Raman spectroscopy of ZnO/ZnS and ZnO/ZnSe nanocomposites prepared by solvothermal microwave synthesis. *Sci. Tech. Bull. Inf. Technol. Mech. Optics.* 2023, Vol. 23(6), p. 1136–1142. DOI: 10.17586/2226-1494-2023-23-6-1136-1142